



Article

Experimental Evaluation of Dynamic Rock Scour Protection in Morphodynamic Environments for Offshore Wind Jackets

Javier Sarmiento ¹, Raúl Guanche ^{1,*}, Arantza Iturrioz ¹, Teresa Ojanguren ², Alberto Ávila ³ and César Yanes ²

¹ IHCantabria—Instituto de Hidráulica Ambiental de la Universidad de Cantabria, Isabel Torres 15, PCTCAN, 39011 Santander, Spain; sarmientoj@unican.es (J.S.); arantza.iturrioz.ezeiza@gmail.com (A.I.)

² Iberdrola Renovables Energía EIMA, c/Tomás Redondo 1, 28033 Madrid, Spain; tojanguren@iberdrola.es (T.O.); cyanes@iberdrola.es (C.Y.)

³ Scottish Power, 1 Tudor St., London EC4Y 0AH, UK; aavila@scottishpower.com

* Correspondence: guancher@unican.es

Abstract: Bottom-fixed offshore wind turbines are generally built on continental-shelf sections that are morphodynamically active due to their shallow depths and severe wave and current conditions. Such sites are commonly protected against scour to prevent the loss of structural stability. Scour protection can be designed using static or dynamic solutions. Designing dynamic protection requires experimental validation, especially for singular or unconventional structures. This article presents an experimental method for the laboratory analysis of scour protection for jacket foundations placed at morphodynamically active sites. The test campaign was conducted within the project East Anglia ONE (UK) as part of the asset owner studies and aimed to evaluate operation and maintenance (O&M) aspects, independent of the contractor's original design assessments. The physical experiments explored morphodynamic changes on the sea bottom and their importance to scour protection, as well as the importance of the history of the wave loads to the deformation of the rock scour protection. This was explored by repeating different cumulative tests, including a succession of randomly ordered sea states (Return Period (RP) 1-10-20-50 years). The experimental results show that the deformation of the rock scour protection was the greatest when the most energetic sea states occurred at the beginning of the experimental test campaign. The maximum deformation was at 5D50 when the first test was also the most energetic, while it was at 3D50 when not included as the first test, yielding a 40% reduction in the scour protection deformation.

Keywords: fixed foundation; wind energy; scour assessment; scour protection



Citation: Sarmiento, J.; Guanche, R.; Iturrioz, A.; Ojanguren, T.; Ávila, A.; Yanes, C. Experimental Evaluation of Dynamic Rock Scour Protection in Morphodynamic Environments for Offshore Wind Jackets. *Energies* **2021**, *14*, 3379. <https://doi.org/10.3390/en14123379>

Academic Editor: Francesco Castellani

Received: 13 May 2021

Accepted: 6 June 2021

Published: 8 June 2021

Publisher's Note: MDPI stays neutral with regard to jurisdictional claims in published maps and institutional affiliations.



Copyright: © 2021 by the authors. Licensee MDPI, Basel, Switzerland. This article is an open access article distributed under the terms and conditions of the Creative Commons Attribution (CC BY) license (<https://creativecommons.org/licenses/by/4.0/>).

1. Introduction

At the end of 2019, the total European offshore wind power capacity was 22,072 MW, which is equivalent to 5047 turbines, according to [1]. The vast majority are bottom-fixed structures. Therefore, many of them are located in morphodynamically active sites. While most structures are monopoles (81.2%), jackets, gravity base foundations, tripods, and tripiles account for 18.5% of wind turbines, and the market share of these structures is expected to continue to increase.

Designing fixed offshore structures in shallow and intermediate waters requires an integrated perspective that considers the interaction between the fluid, the structure, and the seabed.

The presence of obstacles on the seabed modifies the flow velocity and the sediment transport regime. Increasing the velocity pattern may cause scouring on the contours of the foundation [2]. Depending on its location and foundation type, a structure may experience local scour, global scour, or variations of the seabed level [3]. The development of scour may change the resonance frequencies of the foundation [4], in addition to reducing stability and shortening fatigue life [5]. Reaching equilibrium may take weeks, months, years, or

even decades [6]. This period will fundamentally depend on the geometry of the structure, as well as the morphodynamic and meteorological conditions of the site [7]. Scour is usually analyzed in small-scale physical tests [8]. Such tests are particularly necessary for structures with unique geometries and under special morphodynamic conditions [9].

Different strategies can be followed in order to mitigate or prevent scour in offshore wind structures: (a) Free scour development. (b) Preinstallation of scour protection (predicted actions). (c) A combination of (a) and (b), in which free development occurs before the subsequent installation of the scour protection [9]. The strategy selected depends on the metocean condition, soil characteristics, and platform geometry. When alternatives (b) or (c) are selected, different types of protections, such as rocks (riprap), bags of rock/sand/cement, pneumatic, frond mats, and concrete mattresses are currently available [9]. From among all of them, rocks are the most common protection system used against marine scouring. The size, thickness, and extent of the rock scour protection are designed considering the following failure mechanisms [10]: (1) shear failure (external stability), (2) winnowing (internal stability [11]), and (3) edge scour. The stability of the rock scour protection is usually evaluated by means of a set of physical experiments at a reduced scale (i.e., [12] or [13]).

The rock scour protections are often designed by applying solutions that are statically stable [14]. Under this criterion, rocks should remain stable during design storms (no movement is allowed). Static solutions frequently involve the use of very heavy rocks, which are uneconomic and difficult to install in offshore sites [14]. In recent years, dynamic solutions have become more widely used. Such a solution was introduced by [15], where the use of small rocks for rubble mound breakwaters was studied. Dynamic solutions consist of smaller and thicker rocks than those used in static solutions [14]. In dynamic solutions, upper layer deformation is allowed. Dynamic solutions are necessary in locations with strong morphodynamic changes (the presence of sand waves or mega ripples). These solutions can adapt to seabed fluctuation, while static solutions are excessively rigid [9], and small variations in the seabed could induce protection failure.

For monopiles, different formulations can be used to determine the rock size (statically or dynamically stable solutions), such as those proposed in [16–19]. According to [20], the protection extent can be set at around five times the diameter of the pile at sites where morphodynamic changes are limited. However, at morphodynamically active sites, the extension should be estimated by applying the method proposed in [21].

Unfortunately, for structures with more complex geometries, such as gravity base foundations, jackets, or other designs, there is a lack of semi-empirical formulations for validating rock scour protection (dynamically or statically stable). Therefore, the behavior of this type of solution is usually analyzed in small-scale experimental test campaigns, such as that developed in [14].

In the case of jacket foundations, only a few sets of physical experiments are available in the literature. For instance, in [22] the scour depth around a jacket foundation is compared to a monopile foundation through an extensive set of physical experiments. However, there are no open publications that show the behavior of rock scour protection for jacket foundations located in sites with active morphodynamic environments (like the research shown in [23] for monopiles). In this context, the present article aims to deepen the knowledge on the medium to long-term dynamics of rock scour protection for jackets located in sites with active morphodynamic environments. For this purpose, an experimental test campaign was performed at a 1:30 scale in order to evaluate the scour protection behavior of the jackets of East Anglia One (UK, ScottishPower, Iberdrola Group). With the aim of simulating large morphodynamic variations at the target site, the jacket was placed in an artificial sand wave of +3.5 m. The method for sand wave simulation was similar to that shown in [23] for a monopile.

The first objective of the tests was to evaluate the interaction between a sand wave and the rocks, assessing the falling apron phenomenon in order to better estimate potential maintenance operations (i.e., independently of the studies carried out, to validate the

original design). Based on that, the main idea was to assess the behavior of the rocks located in the outer zones of the protection where the sand wave was propagated and eroded. The goal was to create an island of rocks that prevented the lowering of the seabed, a phenomenon associated with medium and long-term morphodynamic changes. The second objective of the tests was to analyze the importance of the history of hydrodynamic loads on the deformation of the dynamic rock scour protection. Normally, dynamic solutions are tested during one or two design storms, disregarding the history of previous and/or subsequent loads. In order to consider the history of hydrodynamic loads, different groups of sea states were simulated. Each test group consisted of the same six sea states with a duration of 3 h, although the order of execution was changed (1-ascending order (from the lowest to the highest energy), 2-descending order (from the highest to the lowest energy), 3-random order). Based on the findings and considering the storms observed during the useful life of the wind park, O&M activities could be scheduled when the scour protection needed repair.

The rest of the paper is organized as follows: Section 2 provides an overview of the case study. Section 3 describes the experimental test campaign, with details of the test facility, the physical model, the experimental set up, the monitoring system, and the methodology. Section 4 presents the technical results. Finally, the main conclusions of this study are presented.

2. Case Study

The reference case used in this article was based on one of the scour protections designed for the foundations of the wind farm East Anglia ONE. The foundation selected is a 3-legged jacket structure connected to piles previously driven on the seabed (Figure 1).

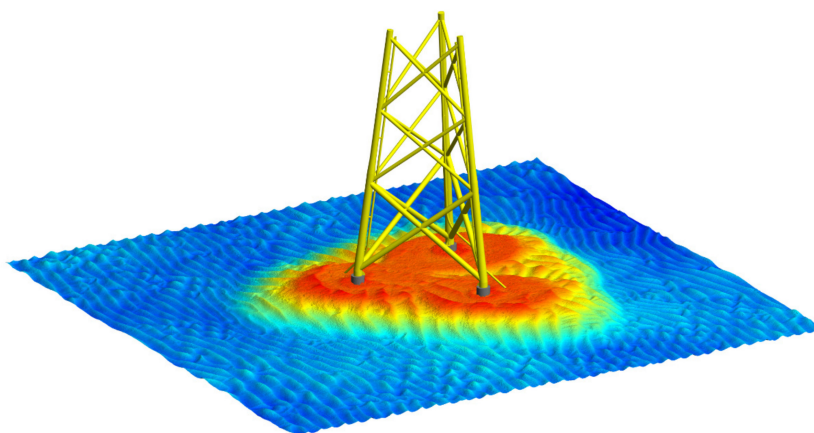


Figure 1. Jacket foundation of East Anglia ONE (laser scanner measurement from physical tests at IHCantabria facilities).

East Anglia ONE is located in the North Sea, approximately 50 kilometers off the coast of the English county of Suffolk (UK). The general bathymetry of the wind farm ranges from 39 to 47 m in depth. The most energetic waves come from the southwest (SW) and north (N), while the predominant currents derive from the northeast and southwest. The seabed consists of a sandy soil typical of the North Sea (surface layers $D_{50} = 0.27$ mm approx.). The relationship between the metocean conditions and the soil properties causes frequent morphodynamic variations at the bottom (i.e., ripples, mega ripples, and sand waves).

Considering the metocean conditions and the properties of the sandy bottom, protections against scour must be installed in order to avoid global and local scour [3].

The extent of scour protection is aimed to adapt to seabed morphodynamic fluctuations (Figure 2). The footprint has an elliptical shape, with the semimajor axis oriented in the predominant direction of the currents and sand wave propagation. The case study evaluates the rock response to the falling apron effect, for a jacket installed on a 3.5 m high

sand wave. The protection should be long enough to cover the full slope of the sand wave once it starts to migrate. The main idea involves a general rock island that avoids the loss of the supporting soil, considered in the design of the pile. [21]. By using this approach, further scour associated with medium-to-long-term morphodynamic changes (such as sand wave propagation or mega ripples [3]) could be avoided.

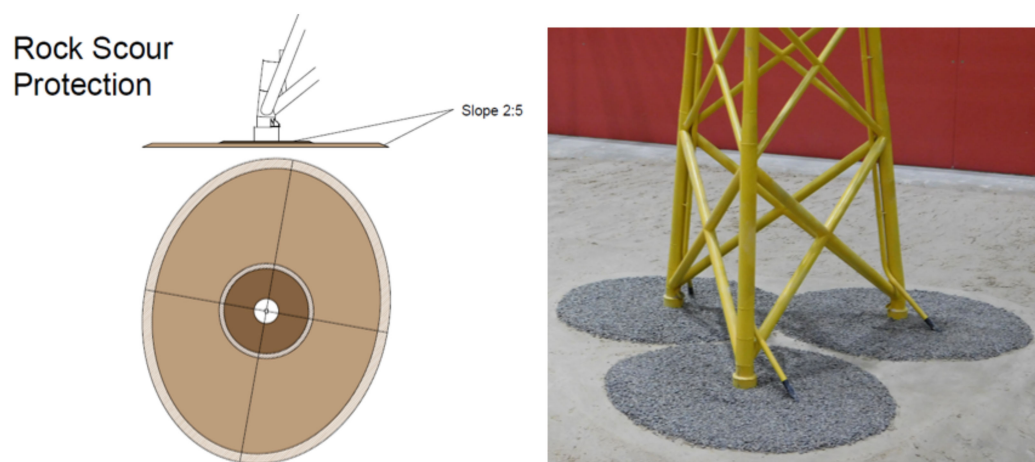


Figure 2. Footprint of the rock scour protection. IHCantabria. Test scale 1:30.

The thickness of the solution was variable. For piles around the jacket (dark brown area in Figure 2, extra increased layer), the thickness was increased by 33% with respect to the areas located away of the piles (light brown areas in Figure 2).

During the experimental tests, the falling apron effect and the stability of the rock in areas adjacent to the three piles were studied.

3. Description of the Experimental Test

3.1. Basin Characteristics

The wave and current tests were performed at the Cantabria Coastal and Ocean Basin (CCOB, Figure 3), managed by IHCantabria (Santander, Spain). The CCOB is 30 m long and 44 m wide, and its maximum water depth is 3 m.

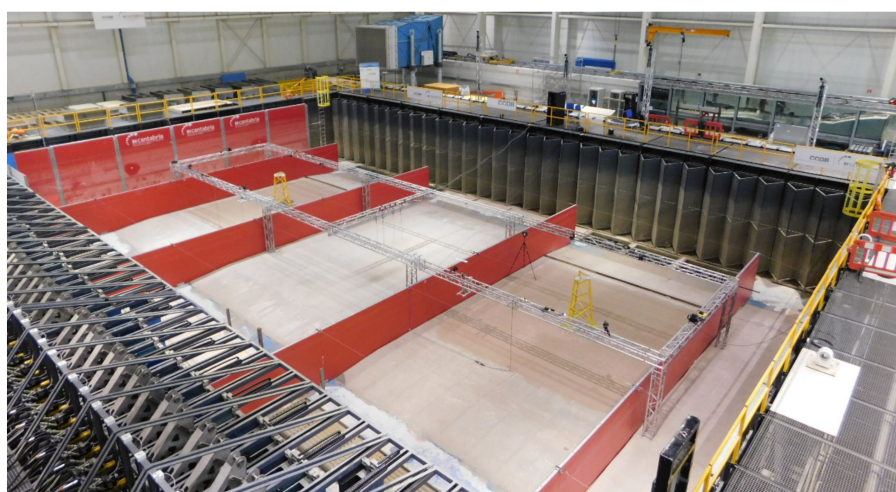


Figure 3. Cont.

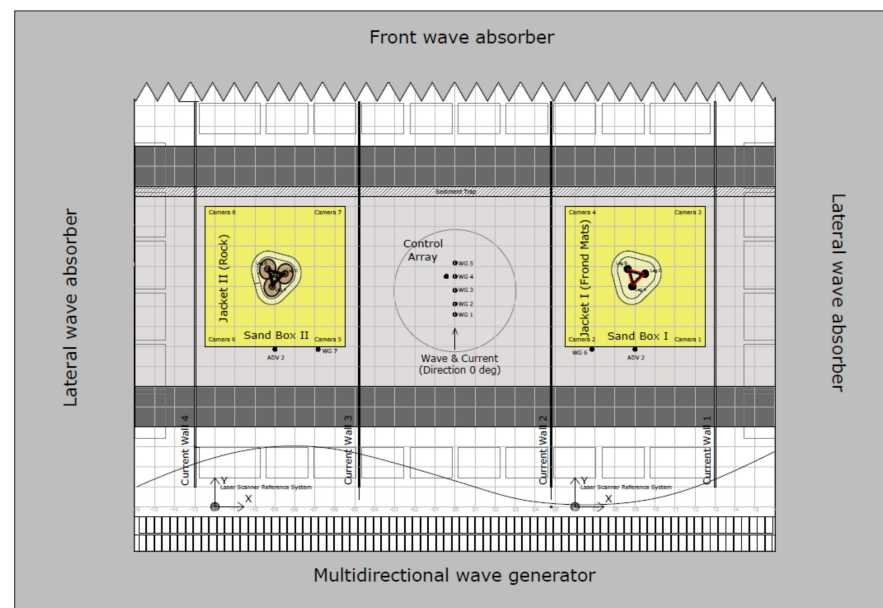


Figure 3. Basin setup.

The tank was divided into three independent channels. Two of these channels were adapted to perform the scour protection tests (see Figure 3). Two structures were tested simultaneously: (1) rock scour protection (described in Section 2), and (2) frond mat protection [24]. Only the rock protection results are presented in this article.

Performing physical experiments with moving sandy bottoms implies adapting a wave–current tank in order to create confined spaces for the sand that would simulate the seabed material. Concrete bathymetry was introduced across the width of the tank to raise the bottom of the tank by 20 cm. In Figures 3 and 4, the interior areas shaded in grey represent the concrete bathymetry, while the areas in yellow were not concreted and were filled with sand. The dimensions of the two sand pits installed in the tank were $7000 \times 7000 \times 200$ mm.

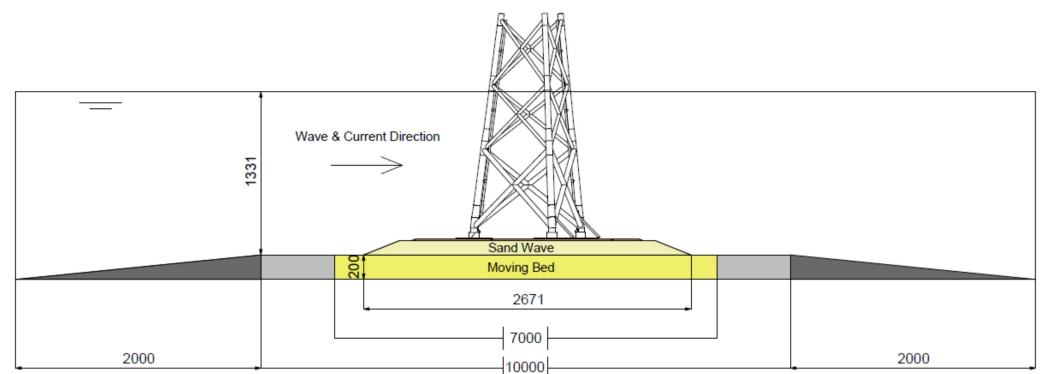


Figure 4. Longitudinal section of the concrete bathymetry (millimeters).

3.2. Experimental Setup

3.2.1. Mock-Up Design

The tests were performed at a 1:30 scale using the Froude similarity law. Granular materials (sand and rock scour protection) were scaled by applying the method proposed in [25].

The physical model was built with steel, including all the elements relevant to the hydrodynamics around the structure, such as j-tubes and the cable protection system (see Figure 5). The structure was rigidly fixed to the bottom to avoid vibrations or unwanted

movements during the tests.



Figure 5. Mock-up.

The rock scour protection was scaled by applying the method proposed in [25] to ensure that the inception of motion was correctly reproduced at both scales.

The sand used for the physical tests had a $D_{50} = 0.17$ mm, while the sand at the site has a $D_{50} = 0.27$ mm. As usual in movable seabed tests, the scale laws described in [25], without adaption, would require cohesive materials at the laboratory scale (D_{50} lower than 0.05 mm), which would not represent the behavior of granular materials. For this reason, the sand selected for the experimental test campaign was the finest available, as recommended by other authors, including [8]. Considering the characteristics of the sand and the selected sea states, the Shields parameter used was always higher than the critical Shields parameter to ensure the propagations of the sand as well as the formation of ripples during the physical experiments [26]. Achieving the same sediment transport at both scales would require distorting the speed of the current. This option was not considered during the experimental tests because all programmed sea states combined the actions of waves and currents.

3.2.2. Test Setup

The jacket was installed at the laboratory according to the field layout. Therefore, the jacket's axis of symmetry was rotated by 15° from the wave and current propagation direction. Moreover, the semimajor axis of the rock scour protection was rotated by 10° from the wave and current propagation direction (Figures 6 and 7).

A sand wave of +3.5 m was included under the rock scour protection (prototype scale, see Figures 6 and 7). The protection was installed on the sand wave, assuming that the top of the protection had a perfectly flat bottom. The simulated sand wave was built as in [23], where a monopile rock scour protection was evaluated.

3.2.3. Test Plan

The test plan included four test groups: (1) individual tests (Table 1), (2) cumulative tests 1, with an ascending sequence ($\times 6$ tests, Table 1), (3) cumulative tests 2, with a descending sequence ($\times 6$ tests, Table 2. Left: Cumulative tests 2, with a descending sequence. Right: Cumulative tests 3, with a random sequence.), (4) cumulative tests 3, with a random sequence ($\times 6$ tests, Table 2).

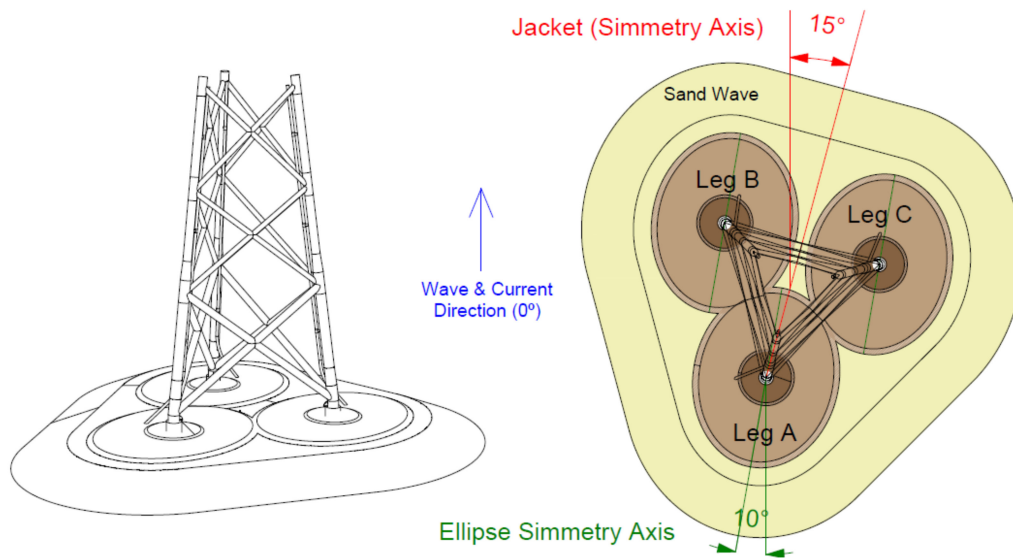


Figure 6. Sketch of Platform orientation, Rock scour protection orientation, and Sand wave orientation.



Figure 7. General view of the test setup.

Table 1. (Left) Individual test. (Right) Cumulative tests 1: ascending sequence.

Tests	Individual Test				Cumulative Tests 1: Ascending Sequence				
	h [m]	Sea State	Currents	Duration (h)	Tests	h [m]	Sea State	Currents	Duration (h)
		RP [yr]	RP [yr]				RP [yr]	RP [yr]	
1	39.93	50	50	3	1	39.93	1	50	3
					2	39.93	5	50	3
					3	39.93	10	50	3
					4	39.93	15	50	3
					5	39.93	20	50	3
					6	39.93	50	50	3

Table 2. (Left) Cumulative tests 2, with a descending sequence. (Right) Cumulative tests 3, with a random sequence.

Cumulative Tests 2: Descending Sequence					Cumulative Tests 3: Random Sequence				
Tests	h [m]	Sea State	Currents	Duration (h)	Tests	h [m]	Sea State	Currents	Duration (h)
		RP [yr]	RP [yr]				RP [yr]	RP [yr]	
1	39.93	50	50	3	1	39.93	15	50	3
2	39.93	20	50	3	2	39.93	1	50	3
3	39.93	15	50	3	3	39.93	5	50	3
4	39.93	10	50	3	4	39.93	50	50	3
5	39.93	5	50	3	5	39.93	10	50	3
6	39.93	1	50	3	6	39.93	20	50	3

The fluctuations of the sand bottom and rock scour protection were measured with a 3D laser scanner (FARO). Measured seabed level differences (final minus initial) are presented in the results section, using the following color scale: (a) white areas show no relative changes between the initial and final conditions, (b) green and blue areas show locations with more material at the end of the test, and (c) yellow and red areas show areas subject to erosion.

4. Results & Discussion

Figures 8 and 9 show the general evolution of the sand wave and the scour protection. The results were divided into two sections: First, the results of the sand wave evolution and its interaction with the rock scour protection (the falling apron behavior) are shown. And second, an assessment of the behavior of the rock protection around the three legs of the jacket (rock stability) is summarized.

4.1. Falling Apron Behavior

First, the falling apron behavior of the system against the scour was analyzed, primarily by focusing on the fall of the material due to sand wave migration. As mentioned above and according to the available literature, such tests have primarily been performed to study monopiles [23].

The results (laser scanner measurement final minus initial condition) are shown in Figure 8 (photographs taken at the end of the four batches) and Figure 9 (laser scanner measurements).

In both figures, the subplot located in the upper left shows the results from the individual test (only one sea state). The other images in Figures 8 and 9 (upper right; lower left and right) show the results after performing the three sequences of cumulative tests (ascending sequence—upper right, descending sequence—lower left, random sequence—lower right, 18 h total duration). The propagation of the ripples along the contours of the sand wave can be identified as a scale effect.

As expected, the comparison between the propagation of the sand wave in the individual test (RP 50 years and a duration of 3 h) and the groups of cumulative tests (18 h of tests) clearly shows that the sand wave was much more eroded after the cumulative tests. Considering that the duration of the cumulative tests and individual tests differed significantly, the falling apron effect was only quantified and evaluated in the groups of cumulative tests (18 h of sea states).

The three sets of cumulative tests (ascending, descending, and random sequences, Figures 8 and 9) clearly show that the erosion patterns are similar.

Considering the asymmetry of the test due to the orientation of the jacket, the sand wave propagation differed markedly along its perimeter. The highest drop in the sand wave was observed in its frontal area (leg A) and on the AC side (right side of the images). Figure 10 shows the longitudinal profiles measured after each of the sea states of Cumulative test #1 (ascending sequence). These longitudinal profiles extend from the axis of leg A to the beginning of the sand wave. At the end of the test sequence, the maximum descent of the sand wave was slightly higher than half its height (red line). At the beginning of the

tests, the slope of the sand wave was approximately 22° ; in contrast, the final slope of the eroded area was approximately 14° by the end of the cumulative set of tests.

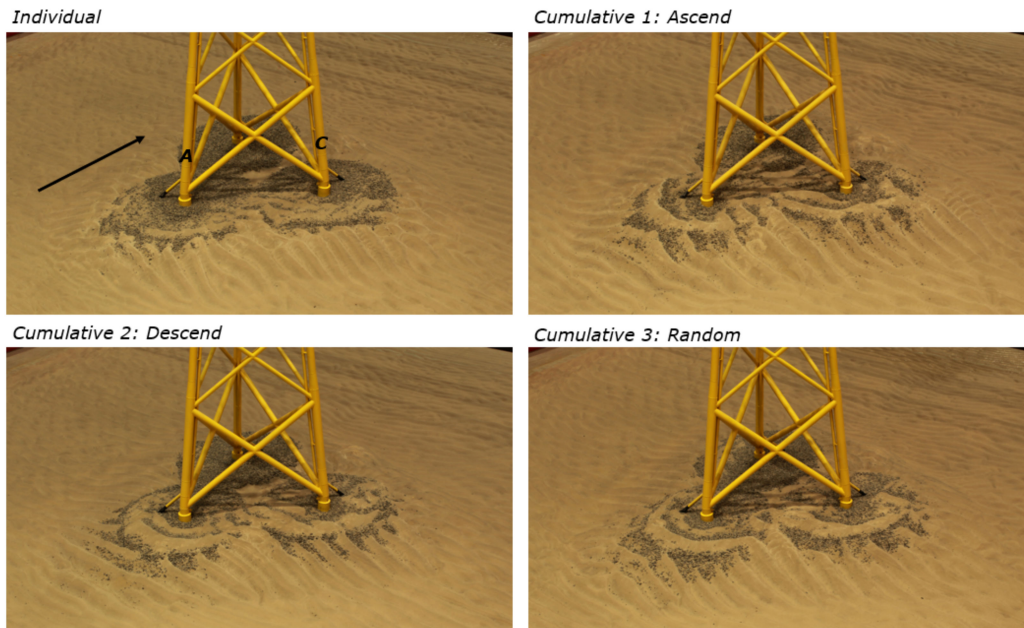


Figure 8. General view of the platform during the tests: **top left:** individual, **top right:** cumulative ascending, **bottom left:** cumulative descending, **bottom right:** cumulative random.

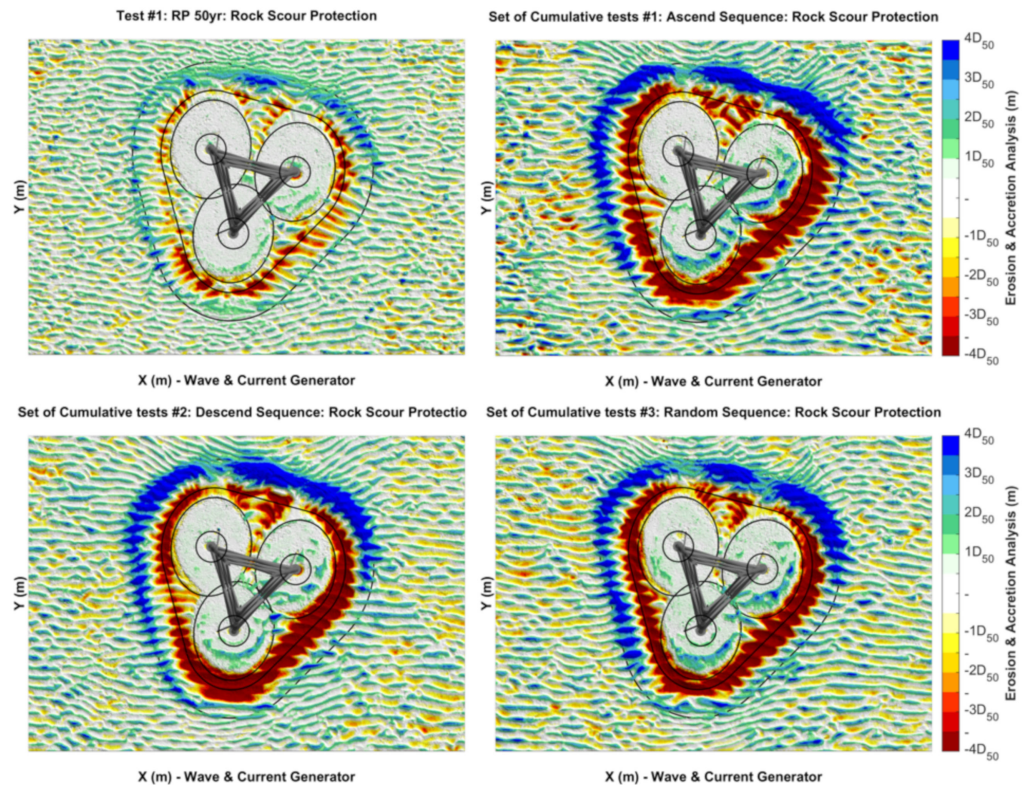


Figure 9. General view of laser scanner measurements: **top left:** individual, **top right:** cumulative ascending, **bottom left:** cumulative descending, **bottom right:** cumulative random.

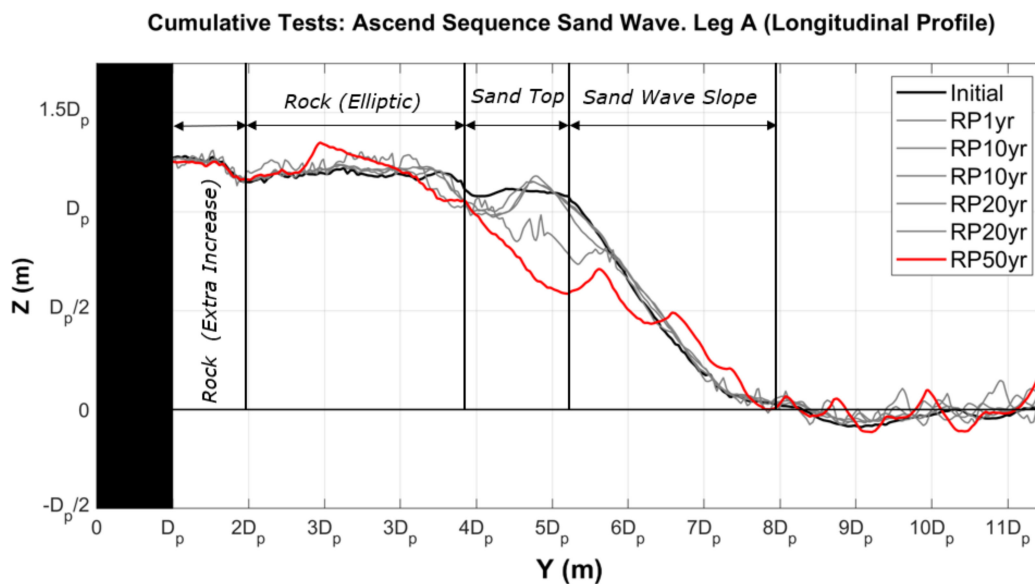


Figure 10. Longitudinal profile from the axis of leg A until the beginning of the sand wave.

For the area with greater sand wave propagation (frontal area of leg A), some rocks of the protection contour were rearranged to the slopes of the eroded sand wave. Due to physical modelling restrictions, tests did not last long enough for the laboratory sand wave to propagate fully. The maximum descent of the rocks along the sand wave covered more than half of its slope, thereby indicating a partial falling apron effect. Visual inspections performed after each set of tests showed that both large and small rocks were found on the slopes of the sand wave. This rock distribution indicates that the protection had behaved as expected, up to that partial migration stage. Authors believe that such rearrangement pattern would have continued for the rest of the sand wave migration.

Lastly, both the sand wave evolution and the rock response to the falling apron were similar in all the groups of cumulative tests. Therefore, scour protection behavior showed low dependency on the hydrodynamic load history from the falling apron point of view.

4.2. Extra Increase Behavior

Once the sand wave evolution and the behavior of the contours of the rock scour protection against the falling apron phenomenon were evaluated, the next step was to analyze the behavior of the protection at the contours of the legs (extra increase, Figure 2 dark brown area). Figures 11–14 show the laser scanner measurements around all three foundation piles.

The maximum erosion was observed around leg C due to the orientation of the jacket and the sand wave during the tests. Both orientations, together with the direction of the waves and currents, induced higher flow velocities in that area.

For leg C, Figure 11 (plan view, leg C), Figure 12 (cross-sectional profile, leg C) and Figure 13 (longitudinal profile, leg C) show the final protection response in the four sets of tests.

At first glance, the variation in both the extent and depth of erosion is highly variable depending on the test set. For the individual waves and the descending sequence of tests, the maximum scour almost reaches a thickness of $5D_{50}$. In turn, in the cumulative ascending and random sequences of tests, the maximum scour is around $3D_{50}$. Therefore, depending on the sequence of tests followed, the difference in the maximum erosion is $2D_{50}$. Thus, considering that $5D_{50}$ was the maximum erosion measured and $3D_{50}$ the minimum, the relative deformation of the rock scour protection could vary up to 40%, depending on the test sequence.

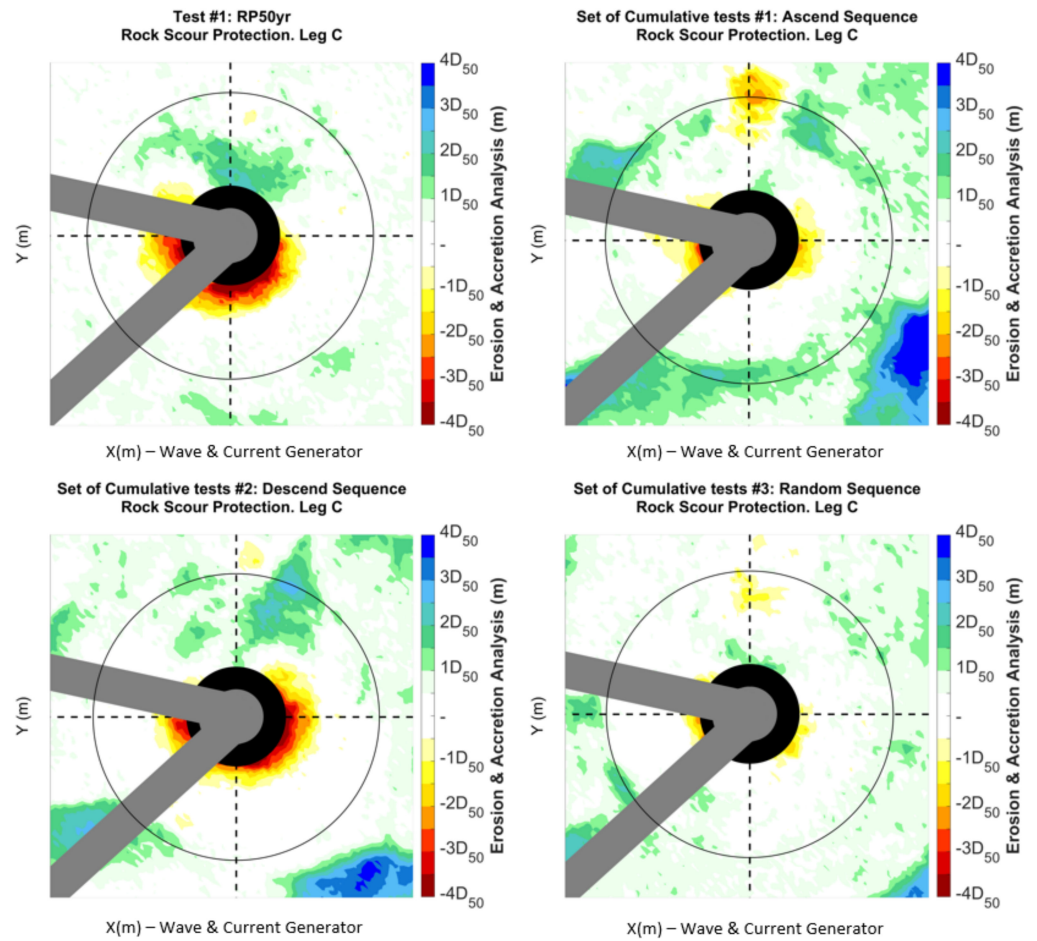


Figure 11. Leg C: extra increase rock protection. **Top left:** individual, **top right:** cumulative ascending, **bottom left:** cumulative descending, **bottom right:** cumulative random.

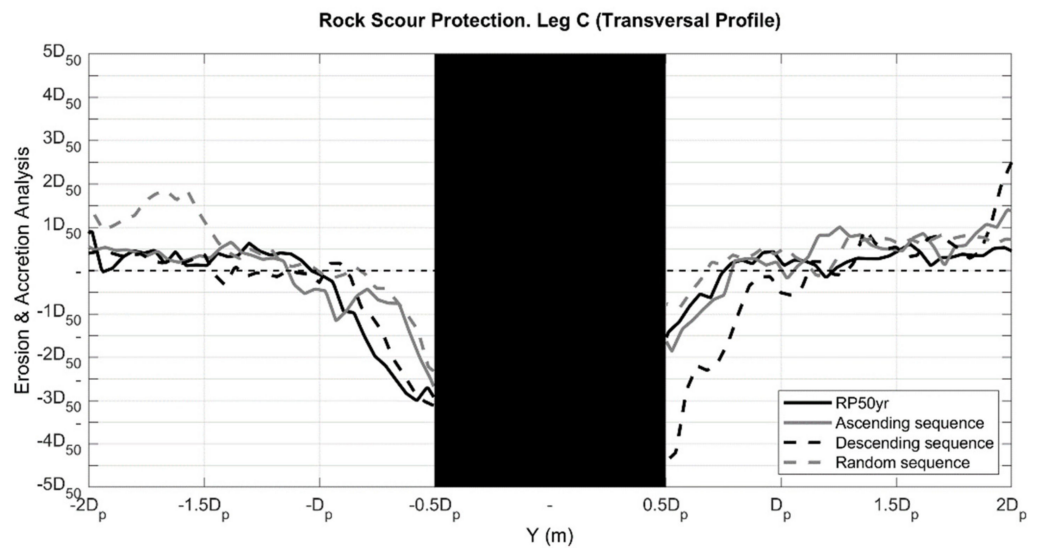


Figure 12. Leg C: cross-sectional profile.

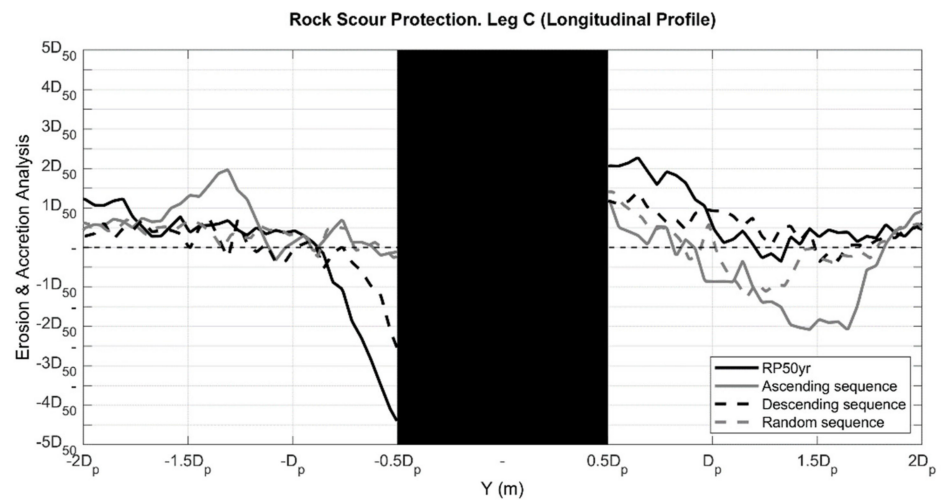


Figure 13. Leg C: longitudinal profile.

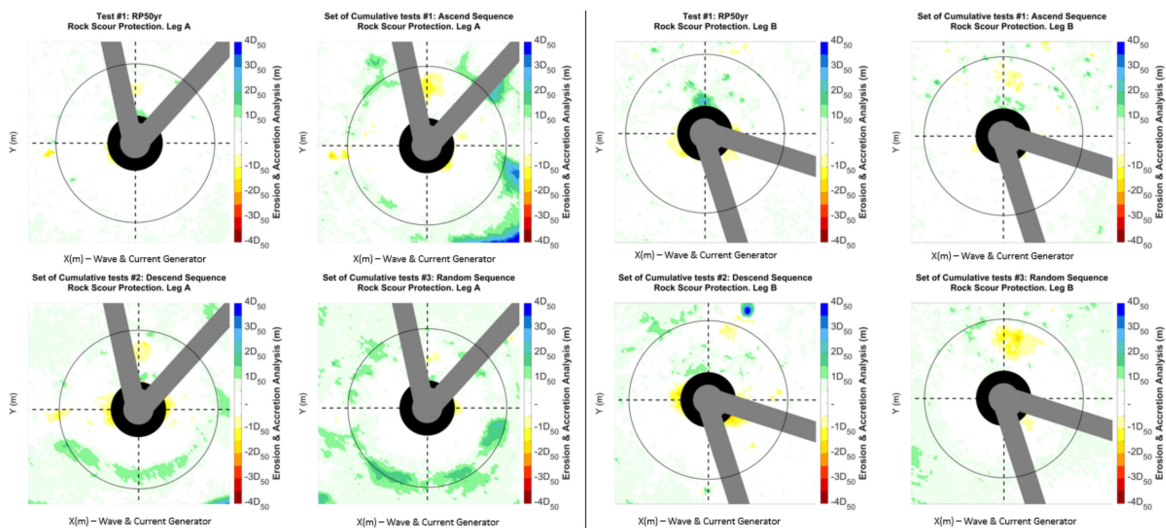


Figure 14. Left: leg A. Right: leg B.

Another aspect that stands out in Figure 11 is the extent of the scour. As with the maximum rock deformation, both the extension at the end of the individual test and that at the end of the cumulative descending sequence cover a larger surface than that observed in the two other groups of cumulative tests (in ascending and random order). For the individual test and the descending sequence of cumulative tests, the eroded surface extends along the entire frontal area of the leg. This erosion is observed in the longitudinal and cross-sectional profiles shown in Figures 12 and 13. These figures show that material eroded from the frontal areas accumulated only in the rear area. Conversely, in the cumulative ascending and random sequences of tests, the eroded surface is located on the lateral contours of the leg (along the cross-sectional profile). Lastly, in all the cases evaluated in this study, the extent of the erosion was approximately 0.5 times the diameter of the pile (from the edge of the leg), being the total extension of the regrown area one pile diameter (from the edge of the leg).

Around legs A and B, Figure 14 shows that the rock movement was very limited. The maximum scour reached $3D_{50}$ only in leg B, with the descending sequence always lower than $2D_{50}$ in all other test groups.

Based on the results observed (mainly around the protection placed around leg C), the order of the sequence of sea states clearly plays a key role in the final deformation of the

rock scour protection. The findings show that if the sea state with the longest return period expected (50 years) occurs at the beginning of the test batch (individual or cumulative descending test batches), the erosion observed in the protection against scour is 40% greater than the values observed when the most energetic sea state occurs at the end or in an intermediate period of the set of tests (cumulative random and ascending order).

5. Conclusions

The processes that trigger scour around offshore jacket structures are complex. As a result, predicting scour is difficult, especially in structures for which the typology causes complicated fluid–structure interactions. This paper described an experimental approach to this problem that focused on the analysis of two aspects: the importance of elements such as sand waves in the behavior of scour protection, and the importance of the hydrodynamic history of environmental loads on scour.

In this study, the foundations of the East Anglia ONE wind farm, which was reproduced in the laboratory at a 1:30 scale at the Cantabria Coastal and Ocean Basin (CCOB) of the Environmental Hydraulics Institute of the University of Cantabria (Instituto de Hidráulica Ambiental de la Universidad de Cantabria—IHCantabria), were studied. The existing morphodynamic changes in the site were simulated by creating an artificial sand wave with a height of +3.5 m. The rock scour protection was seen as a solution that could adapt to the morphodynamic changes expected at the site.

The test plan consisted of four test rounds: one individual test and three sequences of cumulative tests (six tests performed one after the other without reconstructing the damage on the sand bottom, the sand wave, and the rock scour protection). Each batch of cumulative tests comprised a total of six sea states (RP 1-10-10-20-20-50 years). All the tests combined codirectional waves and currents.

The three sequences of cumulative tests were performed by changing the order of the sea states. In the first batch, the sea states were generated in an ascending order (from the lowest to the highest energy); in the second batch, the sea states followed a descending order (from the highest to the lowest energy); and in the third batch, the sea states were run randomly.

The main conclusions are listed below:

- For all groups of cumulative tests, the erosion pattern on the sand wave was similar, regardless of the sequence of tests. The maximum erosion on the sand wave was slightly more than half its height (i.e., equivalent to partial migration of the sand wave). This erosion produced a rearrangement of the rocks, from the contours of the protection to the slope of the sand wave (falling apron). The rearranged contour rocks covered just over half of the slope of the sand wave, starting to give shape to the island of rocks that would prevent the future lowering of the seabed associated with medium- and long-term morphodynamic changes. Once the tests were completed, the rock size distribution on the sand wave slope showed a varied graduation (small and large rocks). This rock distribution indicates that although the falling apron behavior was partially represented, the rocks behaved as expected. In relation to the falling apron effect, the size of the rocks and the extent of the protection tested in this study seem to be adequate.
- In relation to the deformation of the rock scour protection in areas adjacent to the legs of the jacket, the maximum erosion was observed in leg C (up to $5D_{50}$). In leg A, the maximum erosion was $2D_{50}$, and reached $3D_{50}$ in leg B.
- In leg C (where the deformations of the anti-scour protection were at a maximum), the extension and deformation of the rock scour protection differed markedly, depending on the sequence of tests.

When the tests began with the most energetic sea state (individual test or cumulative descending sequence), the deformation of the rock scour protection was much higher than the deformation observed when the most energetic sea state appeared at the end or in the middle of the test sequence (the difference observed between the tests was 40%):

- Group 1: Individual and cumulative descending tests (RP 50 years—first test of the batch): maximum deformation of almost $5D_{50}$ (scour extended approximately 0.5 times the diameter around the entire frontal area of the leg, while eroded rock accumulated behind the leg).
- Group 2: Cumulative ascending and cumulative random tests: maximum deformation of the rock scour protection close to $3D_{50}$. Erosion only occurred on the sides of the leg (along the cross-sectional profile).
- Finally, the maximum erosion in the tests of group 1 (individual or cumulative descending) was 40% higher than the erosion observed in the tests of group 2 (cumulative ascending or cumulative random). The order of the sea states could modify the final rock scour protection deformation.

Based on the results and the case study, the arrival order of storms has a strong effect on the maximum deformation of the scour protection and therefore on the probability of requiring actions during the useful life of the project, depending on the risk assumed in the design. Performing experimental tests following the proposed method (modifying the arrival sequence of the sea states) and monitoring the meteorological conditions during the lifetime of the foundations may help in the programming of corrective O&M operations for protections against scour.

Author Contributions: Conceptualization, R.G. and J.S.; methodology, J.S., R.G. and A.I.; investigation, A.I., R.G. and J.S.; writing—original draft preparation, J.S.; writing—review and editing, R.G. and A.Á.; supervision, A.Á., C.Y. and T.O.; project administration, C.Y. and T.O.; funding acquisition, R.G. and C.Y. All authors have read and agreed to the published version of the manuscript.

Funding: This research was part of the Scour Protection Jacket Project (SPJ) and was carried out with Iberdrola and GITECO. The authors acknowledge financial support from the Regional Government of Cantabria through the R&D program PROYECTOS DE I+D+i EN COOPERACIÓN EN ENERGÍAS RENOVABLES MARINAS-2016 (the RM-16-XX-029). Raúl Guancho also acknowledges financial support from the Ramon y Cajal Program (RYC-2017-23260) of the Spanish Ministry of Science, Innovation and Universities.

Conflicts of Interest: The authors declare no conflict of interest.

References

1. Europe. *Offshore Wind in Europe, Key Trends and Statistics*; Wind Europe: Brussels, Belgium, 2020.
2. Sumer, B.M.; Fredsøe, J. *The Mechanics of Scour in the Marine Environment*; Advanced Series on Ocean Engineering: River Edge, NJ, USA, 2002.
3. Whitehouse, R. *Scour at Marine Structures: A Manual for Practical Applications*; Thomas Telford Limited: London, UK, 1998.
4. Raaijmakers, Q.; Rudolph, D. Time-dependent scour development under combined current and waves conditions -laboratory experiments with only monitoring technique. In Proceedings of the 4th International Conference on Scour and Erosion, Tokyo, Japan, 5–7 November 2008.
5. Boon, D.; Sutherland, J.; Whitehouse, R.; Soulsby, R.; Stam, C.-J.; Verhoeven, K.; Høgedal, M.; Hald, T. Scour behaviour and scour protection for monopile foundations of offshore wind turbines. In Proceedings of the European Wind Energy Conference, London, UK, 22 November 2004; [CD-ROM]. p. 14.
6. Whitehouse, R.J.S.; Harris, J.; Sutherland, J.; Rees, J. The nature of scour development and scour protection at offshore windfarm foundations. *Mar. Pollut. Bull.* **2011**, *62*, 73–88. [[CrossRef](#)] [[PubMed](#)]
7. Whitehouse, R.J.S.; Harris, J.M.; Mundon, T.; Sutherland, J. Scour at offshore structures. In Proceedings of the Fifth International Conference on Scour and Erosion (ICSE-5), San Francisco, CA, USA, 7–10 November 2010.
8. Whitehouse, R.J.S.; Sutherland, J.; O'Brien, D. Seabed Scour Assessment for Offshore Windfarms. In Proceedings of the 3rd International Conference on Scour and Erosion, Gouda, The Netherlands, 1–3 November 2006.
9. Raaijmakers, A.J.A.; Roetert, T.; van Steijn, P. *Scour and Scour Mitigation for Hollandse Kust (Zuid): Recommendations for Foundations and Cables*; Deltares: Delft, The Netherlands, 2017.
10. Hoffmans, G.J.C.M.; Verheij, H.J. *Scour Manual*; A.A. Balkema: Rotterdam, Netherlands, 1997.
11. Sumer, B.M.; Nielsen, A.W. Sinking failure of scour protection at wind turbine foundation. *Proc. ICE Energy* **2013**, *166*, 170–188. [[CrossRef](#)]
12. Mayall, R.O.; McAdam, R.; Whitehouse, R.; Burd, H.; Byrne, B.; Heald, S.; Sheil, B.; Slater, P. Flume tank testing of offshore wind turbine dynamics with foundation scour and scour protection. *J. Waterw. Port Coast. Ocean Eng.* **2020**, *146*, 04020033. [[CrossRef](#)]

13. Wu, M.; de Vos, L.; Chavez, C.E.A.; Stratigaki, V.; Fazerer-Ferradosa, T.; Rosa-Santos, P.; Taveira-Pinto, F.; Troch, P. Large Scale Experimental Study of the Scour Protection Damage Around a Monopile Foundation Under Combined Wave and Current Conditions. *J. Mar. Sci. Eng.* **2020**, *8*, 417. [[CrossRef](#)]
14. de Sonnevile, B.; van Velzen, G.; Wigaard, J. Design and optimization of scour protection for offshore wind platform Dolwin Beta. In Proceedings of the 33rd International Conference on Ocean, Offshore and Arctic Engineering, San Francisco, CA, USA, 8–13 June 2014.
15. Van der Meer, J.W. *Rock Slopes and Gravel Beaches under Wave Attack*; Delft Hydraulics: Delft, The Netherlands, 1988.
16. de Vos, L.; de Rouck, J.; Troch, P.; Frigaard, P. Empirical design of scour protections around monopile foundations. Part 1: Static Approach. *Coast. Eng.* **2011**, *58*, 540–553. [[CrossRef](#)]
17. De Vos, L.; de Rouck, J.; Troch, P.; Frigaard, P. Empirical design of scour protections around monopile foundations. Part 2. Dynamic Approach. *Ocean Eng.* **2012**, *58*, 540–556.
18. Nielsen, A.W.; Petersen, T.U. Stability of cover stones around a vertical cylinder under the influence of waves and current. *Coast. Eng.* **2019**, *154*, 103563. [[CrossRef](#)]
19. Fazerer-Ferradosa, T.; Welzel, M.; Taveira-Pinto, F.; Rosa-Santos, P.; Chambel, J. Brief review on the limit state function of dynamic scour protections. In Proceedings of the 2nd Conference of Computational Methods in Offshore Technology and First Conference of Oil and Gas Technology (COtech & OGtech 2019), Stavanger, Norway, 27–29 November 2019.
20. Whitehouse, R.; Brown, A.; Audenaert, S.; Bolle, A.; de Schoesitter, P.; Haerens, P.; Baelus, L.; Troch, P.; Neves, L.D.; Ferradosa, T.; et al. Optimising scour protection stability at offshore foundations. In Proceedings of the 7th International Conference on Scour and Erosion, Perth, Australia, 2–4 December 2014.
21. Van Velzen, G. *Flexible Scour Protection around Cylindrical Piles*; Delft University of Technology: Delft, The Netherlands, 2012.
22. Welzel, M.; Schendel, A.; Hildebrandt, A.; Schlurmann, T. Scour development around a jacket structure in combined waves and current conditions compared to monopile foundations. *Coast. Eng.* **2019**, *152*, 103515. [[CrossRef](#)]
23. Riezebos, H.; Raaijmakers, T.; Tönnies-Lohmann, A.; Waßmuth, S.; van Steijn, P. Scour protection design in highly morphodynamic environments. In Proceedings of the 8th International Conference on Scour and Erosion, Oxford, UK, 12–15 September 2016.
24. Available online: <https://sscsystems.com/scour> (accessed on 8 January 2021).
25. Hughes, S.A. *Physical Models and Laboratory Techniques in Coastal Engineering*; World Scientific Publishing Co. Pte. Ltd: Singapore, 1993.
26. Soulsby, R. *Dynamics of Marine Sands: A Manual for Practical Applications*; Thomas Telford: London, UK, 1997.